Characteristics of a laser triggered spark gap using air, Ar, CH$_4$, H$_2$, He, N$_2$, SF$_6$, and Xe

W. D. Kimura, M. J. Kushner,[a] and J. F. Seamans

Spectra Technology, Inc., 2755 Northup Way, Bellevue, Washington 98004-1495

A KrF discharge laser (248 nm) has been used to laser trigger, by volume preionization, a spark gap switch (38–65 kV, > 10 kA, 100 ns pulse duration) filled with 20 different gas mixtures using various combinations of air, Ar, CH$_4$, H$_2$, He, N$_2$ SF$_6$, and Xe. A pulsed laser interferometer is used to probe the spark column. Characteristics studied include the internal structure of the column, the arc expansion rate, and evidence of any photoionization precursor effect. Our results show that the rate of arc expansion varies depending on the average molecular weight of the mixtures. In this experiment, pure H$_2$ has the highest rate ($\approx 9.5 \times 10^5$ cm/s) and air has one of the lowest ($\approx 7 \times 10^5$ cm/s) for the same hold-off voltage. A computer model of the spark column formation is able to predict most of the structure observed in the arcs, including the effect of mixing gases with widely different molecular weights. The work suggests that, under proper circumstances, the spark gap switch performance may be improved by using gases lighter than conventional switch gases such as SF$_6$.

I. INTRODUCTION

Laser triggering of high voltage spark gap switches is a method by which controlled, low jitter breakdown can be achieved.[1,2] Laser volume preionization triggering[2-4] (axial mid-gap illumination) of the gas mixture with ultraviolet (UV) laser light is one of several approaches[5,6] for initiating breakdown of the gap. Typically, SF$_6$ is used as the switch gas mixture because of its excellent voltage stand-off properties and because it also has a low breakdown threshold at UV wavelengths.[2,7] Organic additives to the switch gas mixtures have also been studied[7] as a way to improve laser triggering performance; however, they have the disadvantage of being dissociated by the spark and UV laser light, which generally results in coating the interior of the spark chamber with organic products. In addition, these organic additives are often toxic and/or carcinogenic. SF$_6$ also has the disadvantage of coating the inside of the switch chamber with sulfur products resulting from dissociation, which can cover the windows used for the laser beam access unless care is taken to constantly purge the window surfaces. The breakdown products of SF$_6$ are also deleterious and toxic. A less obvious disadvantage with SF$_6$ is that it is a fairly heavy molecule (molecular weight = 146 amu) which hinders the rapid expansion of a spark column and can lead to higher switch loss than if a lighter molecular weight gas is used.[8]

This paper presents results which demonstrate that reliable laser triggering (volume preionization) at 248 nm of a high voltage spark gap switch is possible in a wide variety of gas mixtures, many of which had not been investigated before this study. The gas mixtures studied are summarized in Table I. The mixtures consist of various combinations of air, Ar, CH$_4$, H$_2$, He, N$_2$, SF$_6$, and Xe, with total absolute gas pressures ranging from 0.25 to 3.0 atm. The peak voltage,

V_{peak}, across the spark gap (i.e., the voltage at breakdown) varies from 38 to 65 kV.

Gas mixtures studied during this program were chosen for the following reasons. Those mixtures containing SF$_6$ are of interest for the reasons described above and because SF$_6$ provides a baseline by which the results of this study can be compared to others. Mixtures of SF$_6$ and N$_2$ have also been examined before.[7] Likewise, dry air was studied because it is also a common switch gas and, in addition, contains oxygen which is an electron attaching gas. Helium and H$_2$ were studied because of the interest in possibly improving switch performance by using a gas with a low molecular weight. (Low molecular weight gases have higher sonic velocities, and therefore expand to form the spark channel more rapidly.) Argon and xenon were studied as additives to the gas mixtures. The objective was to use the relatively low ionization potential of these noble gases as a way of possibly accelerating the spark column growth via a photoionization precursor effect. Methane was also tested as an additive because

TABLE I. Gas mixtures and parameter space investigated.

Gas mixtures:	
1. He	11. CH$_4$/H$_2$
2. N$_2$/He	12. Ar/H$_2$
3. H$_2$/He	13. Xe/H$_2$
4. SF$_6$/He	14. Xe/N$_2$/H$_2$
5. SF$_6$/N$_2$/He	15. Xe/CH$_4$/H$_2$
6. Xe/SF$_6$/He	16. Air (dry)
7. Xe/N$_2$/He	17. He/Air (dry)
8. Xe/SF$_6$/N$_2$/He	18. Xe/Air (dry)
9. H$_2$	19. SF$_6$/N$_2$/Ar
10. N$_2$/H$_2$	20. SF$_6$

Total pressures: 0.25–3 atm abs

Peak voltage across gap: 38–65 kV

it is known to have a fairly low breakdown threshold at 248 nm.[9]

Under the proper conditions, most of the gas mixtures listed in Table I can be successfully laser triggered. The fact that these mixtures can be laser triggered with 248-nm light requires a multiphoton ionization process to occur. Since each photon is 5.0 eV, three or four photons are needed to ionize a typical gas molecule. An exception is pure He which could not be laser triggered at 248 nm; however, this mixture was not studied extensively during this program and, under the proper conditions, it may be possible to successfully laser trigger it via resonance enhanced multiphoton absorption. Each mixture has a range of concentrations for its gas constituents for which successful laser triggering can be obtained.

Section II describes the experimental results of our survey of gas mixtures for laser triggering. The predictions from a computer model[10] of the spark column formation are examined in Sec. III. Section IV summarizes the conclusions of this study.

II. EXPERIMENTAL RESULTS

The apparatus used to trigger and study the spark gap has been described elsewhere.[3,11,12] A KrF laser (248 nm) is focused coaxially between two hemispherical copper electrodes separated by 1.2 cm with 1-mm-diam holes in their centers through which the laser beam passes. The laser intensity at the gap is $\approx 3 \times 10^{10}$ W/cm^2. A pulse-forming line delivers 38–65 kV, > 10 kA, 100 ns pulses to the spark gap.

The spark column is located in one branch of a Mach–Zehnder interferometer whose light source is an excimer pumped dye laser. This diagnostic is used to obtain time-resolved interferograms of the arc formation. The interference fringe pattern is imaged onto a vidicon and recorded on video tape for later analysis.

The dye laser of the interferometer, with a pulse length of < 5 ns, probes transversely across the spark column and provides two-dimensional images of the spark column structure. A shot-by-shot temporal history of the evolution of the spark column is obtained by varying the delay time between laser triggering the switch and triggering of the interferometer laser. It should be emphasized that the accurate temporal data obtained during this experiment would not be possible without the use of laser triggering. The low jitter, high reliability, and spatial control provided by laser triggering makes it possible to adjust accurately when the interferometer probe beam illuminates the spark column relative to breakdown and ensures that the spark column forms in the field of view of the interferometer detector system (vidicon camera). When the switch is allowed to self-break, it is difficult to obtain interferograms of the spark due to uncertainties of when and where breakdown will occur.[3]

A. Interpretation of spark column interferograms

Figure 1 is a schematic drawing of a typical fringe shift pattern seen in interferograms of the spark column. The interferometer is adjusted so that fringe shifts in the upward direction correspond to increasing heavy particle density
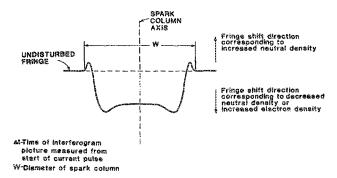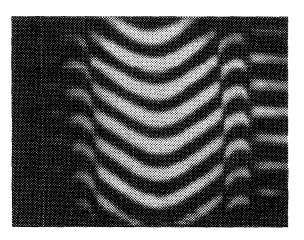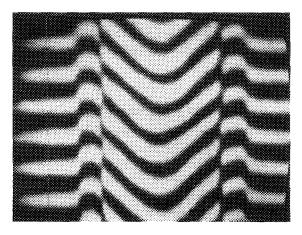

FIG. 1. Schematic drawing of a typical fringe shift pattern from an interferogram of the spark column. The column is oriented vertically.

(i.e., compression of the gas). Fringe shifts in the downward direction then correspond to decreasing heavy particle density (i.e., rarefaction of the gas) or increased electron density.

The fringe shifts caused by the electrons and heavy particles have reciprocal wavelength dependencies; hence, it is possible to separate their contribution to the total fringe pattern by obtaining interferograms at the same time during the arc, but at two different wavelengths. Figure 2 shows an

a) 392.9 nm, w = 0.89 mm

b) 616.0 nm, w = 0.87 mm

FIG. 2. Typical interferograms obtained at two different interferometer wavelengths. The gas mixture is 1% Xe/99% H$_2$ at 2 atm total pressure; $V_{peak} \approx 48$ kV; and $\Delta t = 42$ ns. (a) $\lambda = 3929$ Å; (b) $\lambda = 6160$ Å.

example of interferograms taken under the same conditions, but with two different laser wavelengths. In Fig. 2(a), the laser probe wavelength λ is 3929 Å; in Fig. 2(b) it is 6160 Å. The gas mixture is 1% Xe/99% H_2 at 2 atm abs (all pressures in this paper are absolute) with $V_{peak} \approx 48$ kV. The delay time, indicated by Δt, is the time that the interferogram is obtained after the start of the current pulse. For these examples, $\Delta t = 42$ ns. The diameter of the column measured from the interferogram, indicated by w (see Fig. 1), is ≈ 0.9 mm for both interferograms.
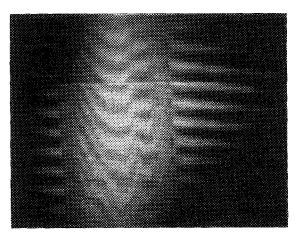
The interpretation of the interferograms is that the spark column consists of a shell of compressed gas, mostly neutral at the leading edge, surrounding a core of high electron density and low neutral density. Note at the longer probe wavelength [Fig. 2(b)], which is more sensitive to electron density, that the center of the column has a greater downward fringe shift indicating a large concentration of electrons in this volume. The fringe shift caused by the heavy particles is more sensitive to the blue wavelengths, and, as expected, the upward fringe shift at the edge of the column is more pronounced in Fig. 2(a). An analysis of the interferograms, such as those depicted in Fig. 2, can yield the electron and heavy particle density profiles.[3]

All the mixtures studied are amenable to dye laser interferometry, except for mixtures with SF_6 concentrations greater than approximately 40%. It is difficult to probe mixtures with a high fraction of SF_6 with the dye laser and obtain any details of the internal structure of the spark column. The relatively high index of refraction of SF_6 and the high electron densities (10^{18}–10^{19} cm^{-3}) inside the spark column when using SF_6 cause the laser light probing the arc to refract away from the column, thereby reducing collection efficiency. This loss of light causes a reduction in resolution of the interferogram. The high electron densities also create very large fringe shifts that are difficult to measure because the fringes become very faint and narrow. Spark columns in SF_6 also emit large amounts of broadband light, and may also absorb a significant amount of the laser probe light. Even with narrow-band filters, it is difficult to distinguish laser light from spark column emission. The net effect is that interferograms of high SF_6 mixtures are essentially schlieren photographs of the spark column. Although details of the interior of the spark column cannot be resolved, the diameter of the column as a function of time can be accurately measured.[3]
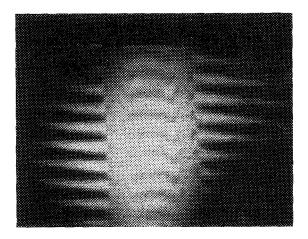
B. Axisymmetric versus chaotic column formation

Three types of spark column formation behavior can be identified. The first is laser triggered arcs that are characterized by axisymmetric columns. The second is laser triggered arcs that often form nonaxisymmetric columns with chaotic internal structures. The third is arcs that are not successfully laser triggered and exhibit chaotic column formation behavior similar to self-breakdown sparks.

The first two behaviors are demonstrated in Fig. 3 which shows interferograms of two different SF_6/N_2/He mixtures. In Fig. 3(a), there is no N_2 in the mixture (the SF_6 is held fixed at 5%) and the resultant spark column

(a) $\Delta t = 112$ nsec, 5% SF_6/0% N_2/95% He

(b) $\Delta t = 97$ nsec, 5% SF_6/10% N_2/85% He

FIG. 3. Dependence on N_2 concentration of spark column formation in SF_6/N_2/He mixtures. The SF_6 concentration is held fixed at 5%. Total pressure is 1.5 atm; $V_{peak} \approx 40$ kV; and $\lambda = 3929$ Å. (a) 0% N_2; (b) 10% N_2.

formation tends to have a chaotic interior structure. When 10% N_2 is added to the mixture [Fig. 3(b)], the spark column formation is consistently axisymmetric.

The chaotic interior structure indicates that breakdown is only laser assisted as opposed to laser triggered. By laser assisted we mean that precursor seed electrons are provided by laser photoionization; however, the spark column is formed from streamers originating from the seed electrons much like self-breakdown. In contrast, laser triggering provides sufficient preionization electrons so that the spark column is formed by a uniform avalanche of an initially axisymmetric column.

With gas mixtures of SF_6/He and N_2/He, the minimum amounts of additives in He needed to achieve reliable laser triggering with consistent axisymmetric column formation are 20% SF_6/80% He and 40% N_2/60% He. Less SF_6 compared to N_2 is required to obtain reliable triggering, in spite of the fact that SF_6 will rapidly attach low-energy electrons. The initial density of photogenerated electrons is therefore likely to be larger in the SF_6/He mixture.

To summarize the results of our study of $SF_6/N_2/He$ mixtures, Fig. 4 shows the SF_6 and N_2 concentrations in helium necessary to achieve axisymmetric column formation. It should be emphasized that all the mixtures tested (except pure helium) can be reliably laser triggered—that is, breakdown is initiated by the preionizer laser and the column appears to be concentric with the laser beam. It is the subsequent axisymmetric or chaotic column formation that is sensitive to the specific composition of these gas mixtures.

Guenther and Bettis[5] have shown the importance of keeping the delay time between the arrival of the laser trigger pulse and the onset of spark breakdown less than the effective laser pulse duration in order to obtain low jitter performance. It is interesting to note that the axisymmetric and chaotic columns have similar delay times. This delay time is of the order of a few nanoseconds and is less than the pulse length of the laser (≈ 5 ns). This may explain why the chaotic columns are still guided and temporally controlled by the laser despite the nonaxisymmetric formation inside the columns.

Little change in the voltage and current characteristics between axisymmetric and chaotic columns is also observed. These preceding observations seem to indicate that spark gaps need only be laser assisted, as opposed to laser triggered (using our definition for laser triggered), to provide useful spark gap triggering.

C. Spark column expansion rate

Gas mixtures such as He/air, CH_4/H_2, He/H_2, and pure H_2 can be reliably laser triggered under essentially the same conditions as the $SF_6/N_2/He$ mixtures. The ability to laser trigger these other mixtures is important because of the flexibility it offers with regard to designing spark gap switches. The differences one sees between these mixtures is the rate of arc expansion, denoted by v. A high expansion rate means the diameter of the column grows quickly and therefore its impedance decreases more rapidly than for a column with a smaller diameter. This behavior reduces the switch loss,[8] making the switch more efficient. Figure 5 shows the spark column diameter as a function of time after the start of the current pulse. These results are for nearly the same voltage at the time of triggering (36–40 kV). Mixtures consisting of lighter molecular weight gases have the highest expan-
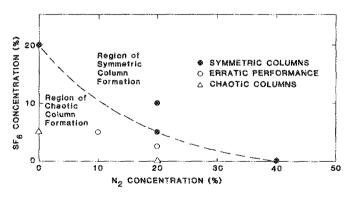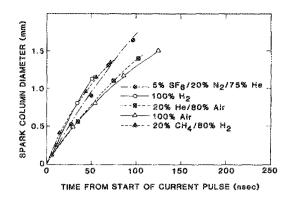
FIG. 5. Dependence of spark column expansion on gas mixture composition. Total pressure is 1.5 atm, $V_{peak} \approx 36$–40 kV.

sion rates. The rates are proportional to the sound speed which scales as $(T_{gas}/M)^{1/2}$. Hence, hot sparks in light gases will have the lowest switch loss. During the first 50 ns, the rate of expansion for air is $\approx 7 \times 10^5$ cm/s, whereas for H_2 it is $\approx 9.5 \times 10^5$ cm/s. Recall that the arc resistance will vary inversely proportional to the area of the column. Therefore, the arc resistance varies as $1/v^2$, and the spark in H_2 can be expected to have only half the resistive loss of the spark in air.

Although using mixtures containing H_2 and He may speed up the arc expansion rate and thereby reduce the switch loss, these gases have lower voltage stand-off capabilities[3] than strong attaching but heavier gases such as SF_6. One must therefore use a higher pressure of the lower molecular weight gas to obtain hold-off. However, this high pressure reduces the arc expansion rate because the increased pressure reduces the specific heating and, therefore, the gas temperature. Fortunately, this reduction in expansion rate is not sufficient to negate the advantage of using lighter molecular gases to reduce switch loss. (The gap separation can also be lengthened to increase hold-off, but this increases the length of the discharge which increases inductance losses.)

The advantages of the light molecular weight gases can be seen more clearly in Fig. 6, which shows the switch loss as a function of the hold-off voltage and the molecular weight of the gas. The curves drawn in Fig. 6 are based upon empirical data obtained on this spark gap device.[8] Note that at a hold-off voltage of 80 kV/cm a pure H_2 mixture must be at 4

FIG. 4. SF_6 and N_2 concentrations in helium buffer mixtures which produce axisymmetric column formation. Total pressure is 1.5 atm and $V_{peak} \approx 40$ kV.
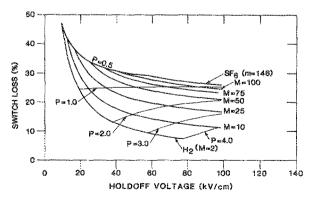
FIG. 6. Scaling map for switch energy loss as a percentage of circuit energy. The average circuit current is 15 kA and the pulse duration is 100 ns.
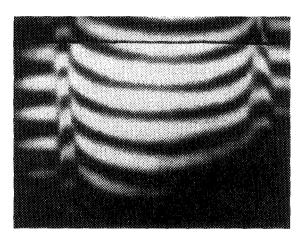
atm, whereas a pure SF_6 mixture must be at less than 1 atm. However, at these pressures the switch loss of the SF_6 mixture is $\approx 27\%$ and the H_2 mixture is only $\approx 7\%$.

From an engineering design point of view, using light molecular weight gases does have the disadvantage of requiring higher pressure switch housings. Issues, such as dealing with mechanical stresses, must be addressed. Therefore, use of light molecular weight gases may be more appropriate in situations where switch losses and/or the need to avoid producing deleterious breakdown products are more critical than mechanical design considerations.
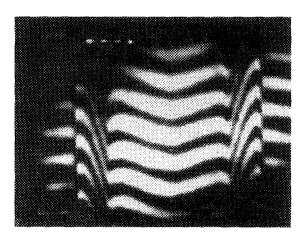
D. Photoionization precursor effect

Gases with low ionization potential, in particular Xe and Ar, were investigated to see if any significant acceleration of the spark column expansion could be induced due to the photoionization of these gases outside the column by UV radiation emitted by the arc.

The effect of adding xenon to H_2 is shown in Fig. 7. Figure 7(a) is a typical interferogram for pure H_2, and Fig. 7(b) is the result of adding 3% Xe to H_2. Comparing Fig.

(a) 100% H_2, Δt = 52 nsec, w = 1.14 mm

(b) 3% Xe/97% H_2, Δt = 50 nsec, w = 1.06 mm

FIG. 7. Effect of adding xenon to hydrogen. Total pressure is 1.5 atm; V_{peak} ≈ 38 kV; and $\lambda = 3929$ Å. (a) No xenon added; (b) 3% Xe added.

7(b) with Fig. 7(a), we see the shape of the column is dramatically changed. Not only is the high density shell wall thicker in Fig. 7(b) than it is in the pure H_2 case, but it has a very different internal structure.

Another difference is that the fringes on the outside of the column no longer appear contiguously straight across the column, but instead seem to be tilting downward away from the column (indicating an upward fringe shift occurring outside the column). This tilted fringe behavior outside the column has only been observed in Xe with either pure H_2, CH_4/H_2, or N_2/H_2 mixtures. The measurements shown in Fig. 7 are at a magnification where it is not possible to observe the full extent of the tilted fringes. Results obtained at a lower magnification, where the fringe shift outside the column can be clearly seen, of a 3% Xe/20% $CH_4/77\%$ H_2 mixture ($V_{peak} \approx 40$ kV, $P = 1.5$ atm) indicate that the curved fringes outside the column extend ≈ 0.22 mm beyond the outer radius of the channel at $\Delta t = 65$ ns. The maximum shift of the curved fringes is approximately one quarter of a fringe space.

The fringe shift outside the column is in the upward direction and is most pronounced at UV wavelengths; this indicates it represents increased gas density or an equivalent effect. This effect is therefore apparently not due to any photoionization precursor although it is still not well understood. It may be due to a thermal expansion wave that precedes the high density shell of the column. As will be discussed in the next section, the primary difference between the pure H_2 and the 3% Xe/97% H_2 mixture is the formation in the xenon mixture of a high density electron shell just interior to the shell of high gas density. This electron shell, which carries a large fraction of the current, may be a heat source that affects the high density gas shell. In any case, no photoionization precursor effect is observed for any of the mixtures or conditions studied during this experiment.

III. MODEL PREDICTIONS

Before discussing some of the model predictions of the spark column formation, the basic characteristics of the interferograms will first be reviewed. Recall that the undisturbed fringe pattern is at the extreme right or left of the interferograms. Upward fringe displacements are due to positive $\Delta\rho/\rho_0$, where $\Delta\rho$ is the change in the gas density and ρ_0 is the initial gas density while downward displacements are due to negative $\Delta\rho/\rho_0$ and electrons. Also recall that the interferogram is a line of sight (LOS) measurement; that is, the probing laser beam transverses across the width of the column, which means the probe light travels through different lengths of the spark column plasma depending on its position with respect to the column center. The LOS data are converted to radially dependent data by performing an Abel inversion.[13]

As noted above, the different appearance of the fringe patterns for a relatively small change in gas mixture is dramatic for Xe/H_2 gas mixtures. In the LOS data of Fig. 7(a) (100% H_2) there appears to be a rather wide but fairly well-defined shell of high gas density. The LOS fringe pattern in the center of the arc appears somewhat circular and is characteristic of a column with a fairly uniform electron density

profile. In the LOS data of Fig. 7(b) (3% Xe/97% H_2) the high gas density region appears to extend further into the column and is less distinct. The fringe pattern in the center of the arc is flatter than that of the pure H_2 mixture and has approximately twice the total shift. The transition to the center plateau occurs steeply in a region close to the high gas density shell. This fringe pattern is characteristic of "heavy" gas mixtures, whereas "light" gas mixtures tend to have the more circular fringe pattern.

Simulated interferograms for the Xe/H_2 mixtures, using results from a previously described computer model,[10] are plotted in Fig. 8. It should be noted that the simulation is for a 1% Xe/99% H_2 mixture, whereas Fig. 7(a) is for 100% H_2; however, the differences in the results are negligible and the conclusions for the 1% Xe mixture also apply to the pure H_2 case. The qualitative agreement between the simulation and the experimental results in Fig. 7 is excellent. The striking difference in the appearance of the fringe pattern is best explained by referring to Fig. 9, where the electron density and the change in gas density, $\Delta\rho/\rho_0$, are plotted as a function of radius for the two cases. For the low xenon case, the electron density, confined within the high mass density shell, is fairly uniform as a function of radius. The electron density penetrates into the high density shell with only a moderate slope. Such a uniform electron distribution will yield a cosinelike LOS fringe pattern in the middle of the column [as seen in Figs. 7(a) and 8]. In contrast, the 3% Xe/97% H_2 case has a high electron density shell interior to the high gas density shell. The LOS fringe pattern is therefore that arising from a shell distribution; it will have a flat center with steep sides. The high gas density shell of the 1% Xe/99% H_2 case is somewhat thinner, but almost a factor of 2 higher than that of the the 3% Xe/97% H_2 case. Mass density in the interior for the low xenon case is rather uniform as opposed to the distribution for the high xenon case which is both higher and has structure.

The differences in shape of the electron density profile, and hence fringe pattern, between the 1% and 3% Xe mixtures results in part from the difference in the average molecular weight of the gas mixtures (3.29 amu versus 5.87 amu), and therefore sound speed. The 1% Xe mixture is sufficient-
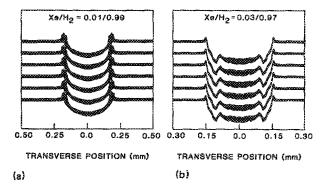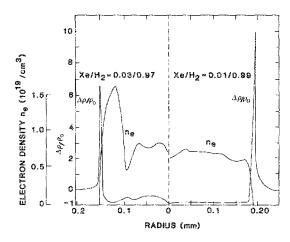

FIG. 9. Profiles of the electron density and the change in gas density for the results given in Fig. 7.

ly light that the gas responds quickly to a pressure gradient. As a result, the convective velocity is positive (radially outward) and the pressure gradient is negative (pressure decreasing radially outward). The molecular weight of the 3% xenon mixture, though, is sufficiently large, and the response time of the gas sufficiently long, that similar conditions cannot be maintained. As a result of the lower convective velocity, the high gas density region just interior to the shell is heated thereby creating a local maximum in pressure. This reverses the pressure gradient, slows the convective velocity interior to the local maximum, and may in fact reverse the particle flux to be radially inward. A local region of low particle density results. This region has a correspondingly higher E/N (electric field divided by gas density) and therefore higher rate of ionization. The result is a shell of high electron density interior to the high gas density shell.

IV. CONCLUSION

Successful laser triggering of 20 different gas mixtures using various combinations of H_2, He, N_2, CH_4, SF_6, Ar, Xe, and air has been demonstrated. The fact that most of these gases are inorganic eliminates the problems associated with organic additives in spark gap devices. Reliable switching can be obtained even when the laser only assists in the formation of streamers (as obtained in self-breaking switches) as opposed to completely forming an axisymmetric spark column. Gas mixtures using lighter molecular weight gases, but having lower hold-off (V/atm) under proper circumstances can yield lower loss switches than heavier, more conventional switch gases.

This work has also shown that subtle changes to the energy transport both inside and outside the spark column can occur in some of these gas mixtures. Although this probably does not directly impact the design of spark gap switches, the data have been very useful in validating a computer model of the spark column formation. This model has been able to predict the formation behavior of the spark, except for the fringe shift seen occurring outside the column in some of the gas mixtures. The cause of this fringe shift is still not entirely understood.

FIG. 8. Simulated interferograms using the computer model developed during this investigation (see Ref. 8). (a) Simulation of the 1% Xe/99% H_2 mixture; (b) simulation of the 3% Xe/97% H_2 mixture. Other conditions are the same as for Fig. 6.

[1] D. R. Humphreys, K. J. Penn, J. S. Cap, R. G. Adams, J. F. Seamen, and B. N. Turman, in *Digest of Technical Papers, 5th IEEE Pulsed Power Conference*, Cat. No. 85 CH2121-2 (IEEE, New York, 1985), p. 262.

[2] W. R. Rapoport, J. Goldhar, and J. R. Murray, IEEE Trans. Plasma Sci. PS-8, 167 (1980).

[3] W. D. Kimura, M. J. Kushner, E. A. Crawford, and S. R. Byron, IEEE Trans. Plasma Sci. PS-14, 246 (1986).

[4] R. G. Adams, D. L. Smith, and J. R. Woodworth, Appl. Phys. Lett. 43, 163 (1983).

[5] A. H. Guenther and J. R. Bettis, J. Phys. D 11, 1577 (1978).

[6] R. A. Dougal and P. F. Williams, J. Appl. Phys. 60, 4240 (1986).

[7] J. R. Woodworth, C. A. Frost, and T. A. Green, J. Appl. Phys. 53, 4734 (1982).

[8] M. J. Kushner, W. D. Kimura, and S. R. Byron, J. Appl. Phys. 58, 1744 (1985).

[9] M. C. Gower, Opt. Commun. 36, 43 (1981).

[10] M. J. Kushner, R. D. Milroy, and W. D. Kimura, J. Appl. Phys. 58, 2988 (1985).

[11] W. D. Kimura, M. J. Kushner, E. A. Crawford, and S. R. Byron, Final report to the Naval Surface Weapons Center, Dahlgren, VA, June 1985 (unpublished).

[12] W. D. Kimura, E. A. Crawford, M. J. Kushner, and S. R. Byron, in *IEEE Conference Record of 1984, 16th Power Modulator Symposium*, Cat. No. 84 CH2056-0 (IEEE, New York, 1984), p. 54.

[13] W. L. Barr, J. Opt. Soc. Am. 52, 885 (1962).